Spectral unmixing using component analysis in multispectral optoacoustic tomography

Stefan Morscher, Jürgen Glatz, Nikolaos C. Deliolanis*, Andreas Buehler, Athanasios Sarantopoulos, Daniel Razansky and Vasilis Ntziachristos
Chair for Biological Imaging & Institute for Biological and Medical Imaging
Technische Universität München & Helmholtz Zentrum München, Munich, Germany

ABSTRACT

Multispectral optoacoustic (photoacoustic) tomography (MSOT) exploits high resolutions given by ultrasound detection technology combined with deeply penetrating laser illumination in the near infrared. Traces of molecules with different spectral absorption profiles, such as blood (oxy- and de-oxygenated) and biomarkers can be recovered using multiple wavelengths excitation and a set of methods described in this work. Three unmixing methods are examined for their performance in decomposing images into components in order to locate fluorescent contrast agents in deep tissue in mice. Following earlier works we find Independent Component Analysis (ICA), which relies on the strong criterion of statistical independence of components, as the most promising approach, being able to clearly identify concentrations that other approaches fail to see. The results are verified by cryosectioning and fluorescence imaging.

Keywords: Photoacoustic tomography, Multispectral Imaging, Spectral unmixing, Blind deconvolution, Independent component analysis, Molecular Imaging

1. INTRODUCTION

Opto-acoustic (or photoacoustic) imaging offers ultrasound resolution based on optical absorption deep in biological tissues[1, 2]. While microscopic applications were under development from the early 80's onwards[3, 4], an increasing interest evolved over the recent years. Tomographic reconstructions allow visualization of deep, light absorbing structures with resolutions up to the micrometer scale. Usage of ultrasound detector arrays recently rendered mechanical movement of the detector unnecessary[5], thus allowing for image generation at much higher speeds even enabling video rate imaging.[6]

Utilizing the advantages of specific optical absorption contrast along different excitation wavelengths enables differential imaging of the bio-distribution of vasculature[7], blood oxygen saturation[8] and biomarkers[9-12]. Especially blood has a sufficiently high optical absorption – and thus generates a large photoacoustic signal – to visualize larger vascular structures in the reconstructed photoacoustic images without any additional tools. For biomarkers the concentration of absorbing molecules that biologically accumulate in targeted tissue (e.g. tumors) is usually lower, thus generating a weaker opto-acoustic signal that may not be distinguishable from the background by the bare eye alone. To a large extent this arises from the high optical density of blood that accounts for large parts of the intrinsic contrast in the image and thus renders necessary the use of advanced methods and tools to visualize the spatial distribution of less optically dense substances. Herein, we present the results from MSOT experiments imaging fluorochrome in deep tissue and examine the performance of three different spectral unmixing methods.

2. METHODS

Optoacoustic measurements were aquired with an MSOT system described in Ref. [6] consisting of a tunable wavelength OPO laser with 10 Hz repetition rate and < 10 ns of pulse duration (Opotek, Inc. Carlsbad, CA) and a 64-element ultrasonic detector array that covers an angle of 172° with center frequency 5 Mhz, (Imasonic SaS, Voray, France). Images were reconstructed using a model-based inversion algorithm that incorporates a model for the detection geometry that enables better image quantity and allows for quantification[13]. After MSOT imaging of the dead corpse, the distribution of Cy7 was imaged using a cryoslicing and epi-illumination imaging system that serves as a gold standard to validate the results by means of fluorescence imaging[14].

*n.deliolanis@helmholtz-muenchen.de

Molecular Imaging III, edited by Charles P. Lin, Vasilis Ntziachristos, Proc. of SPIE-OSA Biomedical Optics,
SPIE Vol. 8089, 80890R · © 2011 SPIE-OSA · CCC code: 1605-7422/11/$18 · doi: 10.1117/12.889415

For this study adult CD1 mice were sacrificed and implanted with an inclusion in the esophagus, after which they were immediately imaged using the described imaging setup. The inclusion consisted of agar and Cy7, a fluorescent contrast agent with an absorption peak around 750nm (measured spectrum see Fig. 2a). The results presented here were achieved using an agent concentration of 5μM in the agar solution, where the concentration was chosen in order for the inclusion not to be visible with the bare eye to demonstrate the performance of the methods presented. Multispectral images were acquired using wavelengths in 5nm steps in a range between 690 and 835nm, allowing a very fine resolution of the absorption spectrum.

The particular goal of this study is to prove that MSOT is capable of revealing the spatial distribution of contrast agents with distinct optical absorption. A key issue in this case is the absorption of tissue, where the main absorbers in the near infrared is hemoglobin. Depending on the amount of oxygen bound its spectral absorption changes greatly from a generally falling slope to a rising slope as up to four oxygen molecules are bound. In the experiments presented here, however, this does not play a big role as the animal is dead, with almost all hemoglobin present being deoxygenated and thus the falling slope dominating the tissue absorption. Still the falling slope present at all available wavelengths forbids the use of simple approaches such as image subtraction that are commonly used in other optical imaging modalities, because even with a steep slope in the absorption profile of a contrast agent the resulting image would still contain a certain amount of signal that is attributed to hemoglobin.

Three more sophisticated approaches to separate absorbers in multispectral imaging that have been introduced in [19] will be examined in the following. Generally the problem of separate absorbers in multispectral imaging is characterized by the equation

$$M = SC,$$

with M being the matrix of measured images. Each line in C is again an image that shows the spatial distribution of an absorber with its spectral profile in the corresponding column of S.

Spectral fitting is a simple and straightforward approach to pursue spectral unmixing given a known set of spectra. The matrix S containing the spectral profiles of absorbers suspected in the sample are inverted using the Moore-Penrose pseudo inverse and multiplied onto the measured images in M. A number of more complex algorithms for matrix factorization and multivariate data analysis have been suggested in literature[15-17] and evaluated for their applicability in optoacoustics.

Two of the most promising methods are Principal Component Analysis (PCA)[16] and Independent Component Analysis (ICA)[17] which will be evalutated here. PCA decomposes data into components that are statistically uncorrelated by finding a set of new basis vectors (principal components) that maximize variance. This can be mathematically computed either by a singular value decomposition or an eigenvalue decomposition of the covariance matrix of the data. Using the newly found base vectors, the measured data can be represented in another coordinate system, where C contains the image representation of the information along the respective base vector. A key advantage of this approach is its automatic sorting of components by variance and thus importance, enabling it also as a possible means of dimension reduction.

ICA pursues a similar approach based on statistical independence by finding directions in the data that represent maximum non-gaussianity under the hypothesis that these directions also represent the maximum information. We used the FastICA algorithm[18] that iteratively maximizes non-gaussianity using kurtosis, which according to the central limit theorem maximizes statistical independence of the components. Again the measurements expressed in the space defined by the newly found base vectors, that can be interpreted in this case as absorption spectra, form the component images in C that represent the distribution of the absorber.

3. RESULTS AND DISCUSSION

Representative reconstructed images acquired at different wavelengths are displayed in Fig. 1a–c. The signal change due to variable absorption of the inclusion across wavelengths is very small and it is not visible even after contrast adjustment or thresholding. This inability demonstrates the necessity of spectral unmixing techniques that are nevertheless able to reveal the contrast agent distribution. Presence and location of fluorescence of the dye are clearly identified in the cryosection RGB and fluorescent images (Fig. 1d-e). A fluorescing straw was being added as a reference to quantify the fluorescent signal in the sample.

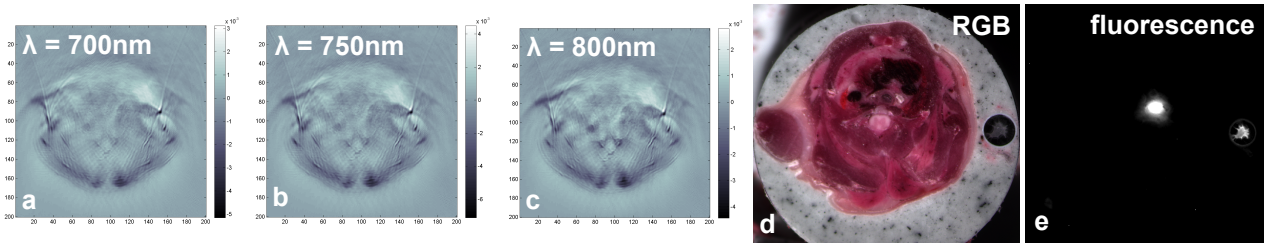

Figure 1. a-c) Representative optoacoustic tomographic reconstructions of the mouse torso at 700nm, 750nm and 800nm respectively d) RGB Image of Cryosection e) Fluorescence Image of Cryosection

Although being a viable approach for more superficial applications, spectral fitting using the Cy7 spectrum measured by the spectrometer (see Fig. 2a; peak absorption μ_a = 2.3 cm^{-1}, 1 cm^{-1} O.D) proved to be unable to resolve the given concentration of contrast agent in deep tissue (see Fig. 2b). The main reason is that light attenuation is variable over wavelengths and thus the spectral profile of light fluence in deep tissue is practically unknown. As a result, the spectral variation of optoacoustic signals does not match with the known absorption spectrum of the fluorochromes used in spectral fitting.

Processing with PCA produced component images, one of which contained the inclusion. This is possible because the uncorrelatedness is still given at increasing depth. Although PCA decomposes a set of cross-wavelength images into the same amount of components ordered by their variance, in general only few of the components actually contain recognizable structures, which is the reason why the contrast is comparatively low.

Finally, unmixing with ICA performed best and the inclusion is clearly identified (Fig. 2e). The superior performance is attributed to the fact that the underlying criterion of statistical independence of the components is stronger than the uncorrelatedness criterion used by PCA. This creates a larger variety of non-noise components and results in clearer spectra of the recovered components. It can be observed in Fig. 2a that the spectrum recovered by ICA (red line) has a left-shifted absorption peak compared to the spectrometer measurements (blue line) for the fact that light fluence in deep tissue is influenced by background absorption.

Optoacoustic tomography is emerging as a high resolution deep tissue biomedical imaging method and especially multispectral acquisitions can serve to identify the biodistribution of various absorbers. Post-processing of the data requires a robust spectral unmixing algorithm and blind unmixing with ICA is shown to perform best, boosting the detection sensitivity of MSOT beyond the limits of the differential or fitting based unmixing methods.

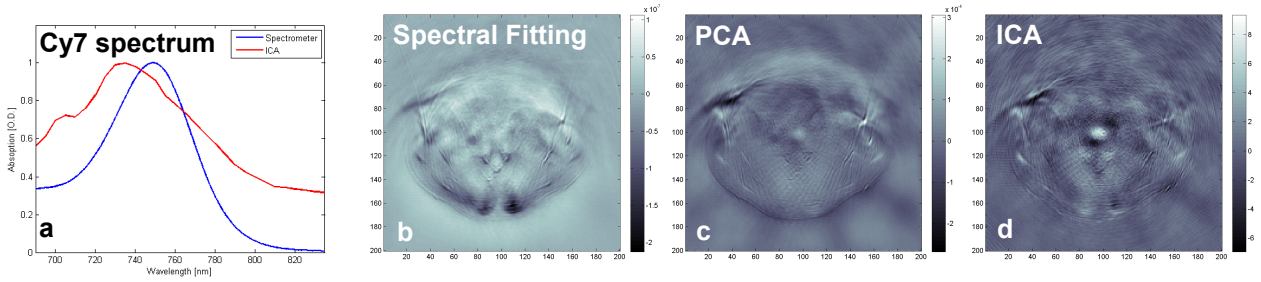

Figure 2. a) Cy7 Absorption spectrum as recorded by the spectrometer (blue line) and as recovered by the ICA unmixing (red line) b) Unmixed Images using Spectral Fitting c) PCA and d) ICA.

REFERENCES

[1] Wang, X. D., Pang, Y. J., Ku, G. *et al.*, "Noninvasive laser-induced photoacoustic tomography for structural and functional in vivo imaging of the brain," Nature Biotechnology, 21(7), 803-806 (2003).

[2] Zhang, H. F., Maslov, K., Stoica, G., and Wang, L. H. V., "Functional photoacoustic microscopy for high-resolution and noninvasive in vivo imaging," Nature Biotechnology, 24(7), 848-851 (2006).

[3] Rosencwaig, A., "Potential clinical applications of photoacoustics," Clin Chem, 28(9), 1878-1881 (1982).

[4] Busse, G., and Rosencwaig, A., "Subsurface imaging with photoacoustics," Appl. Phys. Lett., 36(10), 815-816 (1980).

[5] Brecht, H. P., Su, R., Fronheiser, M. *et al.*, "Whole-body three-dimensional optoacoustic tomography system for small animals," Journal of Biomedical Optics, 14(6), - (2009).

[6] Buehler, A., Herzog, E., Razansky, D., and Ntziachristos, V., "Video rate optoacoustic tomography of mouse kidney perfusion," Opt. Lett., 35(14), 2475-2477 (2010).

[7] Hoelen, C. G. A., de Mul, F. F. M., Pongers, R., and Dekker, A., "Three-dimensional photoacoustic imaging of blood vessels in tissue," Opt. Lett., 23(8), 648-650 (1998).

[8] Wang, X., Xie, X., Ku, G., Wang, L. V., and Stoica, G., "Noninvasive imaging of hemoglobin concentration and oxygenation in the rat brain using high-resolution photoacoustic tomography," J Biomed Opt, 11(2), 024015 (2006).

[9] Ntziachristos, V., and Razansky, D., "Molecular imaging by means of multispectral optoacoustic tomography (MSOT)," Chemical Reviews, 110(5), 2783-2794 (2010).

[10] Taruttis, A., Herzog, E., Razansky, D., and Ntziachristos, V., "Real-time imaging of cardiovascular dynamics and circulating gold nanorods with multispectral optoacoustic tomography," Opt. Express, 18(19), 19592-19602 (2010).

[11] Li, P.-C., Wang, C.-R. C., Shieh, D.-B. *et al.*, "In vivo photoacoustic molecular imaging withsimultaneous multiple selective targeting using antibody-conjugated gold nanorods," Opt. Express, 16(23), 18605-18615 (2008).

[12] Razansky, D., Distel, M., Vinegoni, C. *et al.*, "Multispectral opto-acoustic tomography of deep-seated fluorescent proteins in vivo," Nature Photonics, 3(7), 412-417 (2009).

[13] Rosenthal, A., Razansky, D., and Ntziachristos, V., "Fast semi-analytical model-based acoustic inversion for quantitative optoacoustic tomography," IEEE Trans Med Imaging, 29(6), 1275-85.

[14] Sarantopoulos, A., Themelis, G., and Ntziachristos, V., "Imaging the Bio-Distribution of Fluorescent Probes Using Multispectral Epi-Illumination Cryoslicing Imaging," Molecular Imaging and Biology, 1-12.

[15] Cichocki, A., Zdunek, R., Phan, A. H., and Amari, S.-i., [Nonnegative Matrix and Tensor Factorizations: Applications to Exploratory Multi-way Data Analysis and Blind Source Separation] Wiley, (2009).

[16] Jolliffe, I. T., [Principal Component Analysis] Springer, (2002).

[17] Hyvärinen, A., Karhunen, J., and Oja, E., [Independent Component Analysis, Adaptive and Learning Systems for Signal Processing, Communications, and Control] Wiley InterScience, (2002).

[18] Hyvarinen, A., "Fast and robust fixed-point algorithms for independent component analysis," Ieee Transactions on Neural Networks, 10(3), 626-634 (1999).

[19] Glatz, J., Deliolanis, N. C., Buehler, A., Razansky, D., Ntziachristos, V., "Blind source unmixing in multispectral optoacoustic tomography," Optics Express, Vol. 19, Issue 4, pp. 3175-3184 (2011)